

# Nanostructured Thermosetting Epoxy Systems Modified with Poly(isoprene-*b*-methyl methacrylate) Diblock Copolymer and Polyisoprene-Grafted Carbon Nanotubes

Leandro H. Espósito, José A. Ramos, Iñaki Mondragon, Galder Kortaberria

Materials + Technologies' Group, Department of Chemical and Environmental Engineering, Polytechnic School, University of the Basque Country, Pza. Europa 1, 20018 Donostia-San Sebastian, Spain

Correspondence to: G. Kortaberria (E-mail: galder.kortaberria@ehu.es)

**ABSTRACT:** Nanostructured thermosetting composites based on an epoxy matrix modified with poly(isoprene-*b*-methyl methacrylate) (PI-*b*-PMMA) block copolymer were prepared through PI block segregation. Morphological structures were examined by means of atomic microscopy force microscopy. As epoxy/pristine multi-walled carbon nanotubes (MWCNT) systems were found to present big agglomerations, with a very poor dispersion of the nanofiller, epoxy/PI-*b*-PMMA/MWCNT systems were prepared by using polyisoprene-grafted carbon nanotubes (PI-*g*-CNT) to enhance compatibility with the matrix and improve dispersion. It was found that the functionalization of MWCNT with grafted polyisoprene was not enough to totally disperse them into the epoxy matrix but an improvement of the dispersion of carbon nanotubes was achieved by nanostructuring epoxy matrix with PI-*b*-PMMA when compared with epoxy/MWCNT composites without nanostructuring. Nevertheless, some agglomerates were still present and the complete dispersion or confinement of nanotubes into desired domains was not achieved. Thermomechanical properties slightly increase with PI-*g*-CNT content for nanostructured samples, whereas for nonnanostructured epoxy/PI-*g*-CNT composites they appeared almost constant and even decreased for the highest nanofiller amount due to the presence of agglomerates. Compression properties slightly decreased with block copolymer content, while remained almost constant with nanofiller amount. © 2012 Wiley Periodicals, Inc. *J. Appl. Polym. Sci.* 129: 1060–1067, 2013

**KEYWORDS:** copolymer; nanotubes; graphene and fullerenes; thermosets

Received 4 April 2012; accepted 27 October 2012; published online 23 November 2012

**DOI:** 10.1002/app.38782

## INTRODUCTION

Nowadays, many research studies on the formation of ordered nanostructures in epoxy thermosets containing diblock and triblock copolymers can be found in the literature.<sup>1–6</sup> Interesting properties are expected in the case of composite materials based on matrices nanostructured with block copolymers containing well-dispersed nanoparticles, especially carbon nanotubes (CNT).<sup>7–11</sup> One of the block copolymers that has received considerable interest is poly(isoprene-*b*-methyl methacrylate) (PI-*b*-PMMA),<sup>12,13</sup> which offers new attractive applications in nanoscience and technology.<sup>14</sup> This block copolymer combines the strength and rigidity of PMMA block, miscible with the thermosetting matrix,<sup>2,15</sup> as well as the flexibility of the immiscible PI block. The effect of toughening by the addition of block copolymers with a rubbery block maintaining the transparency of the nanocomposites has been widely published in the literature.<sup>16–19</sup>

On the other hand, as a result of their technological relevance, the use of CNT has received much attention since their discovery due to their unique properties and potential applications

such as remarkable strength and stiffness and superior electrical and thermal conductivity.<sup>20</sup> An adequate CNT dispersion is required for the improvement of properties, as their agglomeration due to the highly attractive forces between them can be therefore minimized. The performance between inorganic nanoparticles as CNT and polymer matrix has been improved with the use of CNT with the polymer grafted onto their surface, avoiding their aggregation.<sup>21–23</sup>

The purpose of this work is to investigate the formation of nanostructures in epoxy thermosets containing PI-*b*-PMMA block copolymer and evaluate the effects of polyisoprene-grafted carbon nanotubes (PI-*g*-CNT) addition on the morphological, thermomechanical, and mechanical properties of the composites.

## EXPERIMENTAL

### Materials

A linear diblock (PI-*b*-PMMA) copolymer, with 78 wt % PMMA was used. It was synthesized by the Department of Materials Science and Engineering of the University of Ioannina,

with a number-average molar mass of  $77,500 \text{ g mol}^{-1}$ . The standards required for anionic copolymerization have been described elsewhere.<sup>24</sup> The epoxy monomer used, diglycidyl ether of bisphenol-A (DGEBA), DER 332, was purchased from Dow Chemical (Midland, MI). It has an epoxy equivalent of around 175. The hardener used was an aromatic amine, 4,4'-methylenebis(3-chloro-2,6-diethylaniline) (MCDEA), supplied by Lonza (Basel, Switzerland). PI-g-CNT were obtained by modifying commercial CNT (Arkema, Lacq, France, diameter 10–15 nm, length 1–10  $\mu\text{m}$ ) in the Department of Materials Science and Engineering of the University of Ioannina. The number-average molecular weight of grafted PI was  $11,000 \text{ g mol}^{-1}$ , and it represented the 20 wt % of the PI-g-CNT. The paste formed was washed and filtrated several times with toluene using polytetrafluoroethylene (PTFE) filters (Waters Corporation, Milford, MA). The material was poured into a petridish and placed into a vacuum oven at  $120^\circ\text{C}$  overnight for solvent removal.

### Blending Protocol

Epoxy/PI-*b*-PMMA/PI-g-CNT composites were prepared in the following way. Different weight percentages of PI-*b*-PMMA, DGEBA, and PI-g-CNT were dispersed in toluene and sonicated for 4 h in a water bath to improve mixing of components. To reduce the entanglements, ultrasonication (Vibracell 75043, Sonics & Materials, Inc., Newtown, CT) was applied for 1 h at room temperature. The resultant mixture was heated at  $110^\circ\text{C}$  under vacuum overnight (12 h) to complete air and solvent removal. MCDEA curing agent was then added at  $110^\circ\text{C}$  and stirred for 5 min. The mixture was then cast into a cylinder mould and cured at  $140^\circ\text{C}$  for 24 h and post cured at  $165^\circ\text{C}$  for 2 h. The same procedure was used for preparing neat epoxy/PI-*b*-PMMA systems.

### Characterization Techniques

Atomic force microscopy (AFM) topography and phase images were recorded in tapping mode (TM-AFM) in air at room temperature by using a scanning probe microscope (Nanoscope IV, Dimension 3100 from Digital Instruments, Santa Barbara, CA). Phosphorus (n) doped single-beam cantilever (125- $\mu\text{m}$  length) silicon probes having a tip with a nominal radius of curvature of 5–10 nm were used. Typical scan rates during recording were 1 line per second. Samples from cured mixtures were prepared using an ultramicrotome (Leica Ultracut R, Viena, Austria) equipped with a diamond knife. Analytical treatment of images was carried out with the public domain ImageJ software.

Dynamic mechanical analysis (DMA) was carried out with a Perkin-Elmer DMA7 (Norwalk, CT) in three-point bending mode to obtain storage modulus ( $E'$ ) and loss factor ( $\tan \delta$ ). Scans were performed at a frequency of 1 Hz and a heating rate of  $5^\circ\text{C min}^{-1}$ , using a span of 5 mm. Parallelepipedic samples ( $12 \times 3 \text{ mm}^2$ ) with a thickness of 1 mm were prepared using cylindrical molds (50 mm height with a diameter of 8 mm), in which the liquid mixture was placed transversely to cure in the oven. After curing, obtained samples were cut to obtain desired dimensions. During the scans, the samples were subjected to a static force of 110 mN and a dynamic force of 100 mN.

Mechanical behaviour of composites was determined using an Instron (Bucks, United Kingdom) Model N<sup>o</sup> 4206 universal testing machine operated in compression mode at room tempera-

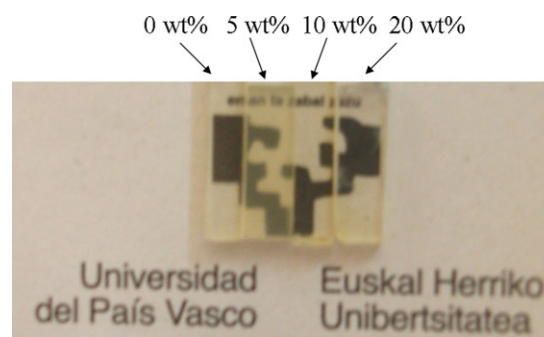


**Figure 1.** Photographs for DGEBA/MCDEA systems modified with different PI-*b*-PMMA contents. Sample thickness: 1 mm. [Color figure can be viewed in the online issue, which is available at [wileyonlinelibrary.com](http://wileyonlinelibrary.com).]

ture. At least five rectangular beam specimens (obtained with cylindrical molds of 6.5 mm of diameter and a height-to-diameter ratio of 1:1) were tested using and a speed of testing according to ASTM D 695-02 standard. Both the top and the bottom of the specimen were prepared with smooth and parallel surfaces perpendicular to the cylindrical axis. They were covered with molybdenum lubricant to avoid friction and barrelling effects.

## RESULTS AND DISCUSSION

### Morphology of Nanocomposites

Transparency observation is a practical way to diagnose at a first glance the compatibility in polymer blends as its existence implies homogeneity on a scale of tens of nanometers or smaller. A macrophase-separated sample is opaque, whereas miscible and ordered samples structured at nanometric scale are transparent. Before and after curing, it was seen that all the epoxy/PI-*b*-PMMA mixtures remained homogeneous and transparent, as shown in Figure 1, suggesting miscibility or development of morphologies by microphase separation in the epoxy matrix. The absence of macrophase separation was also confirmed by optical microscopy (images not shown here).

Several amounts of PI-*b*-PMMA were added to DGEBA/MCDEA thermosetting matrix to achieve nanostructured samples. The morphological structures of DGEBA/MCDEA thermosets containing different amounts of PI-*b*-PMMA were examined by means of AFM. As shown in Figure 2, PI-*b*-PMMA formed microphase-separated domains which were dispersed in a continuous crosslinked epoxy matrix where PMMA subchains remained miscible.<sup>2,15</sup> The spherical-shaped micelle nanodomains were ascribed to PI chains. It has to be noted that the number and the size of spherical nanodomains, and consequently the volume fraction of the separated phase increased with increasing PI-*b*-PMMA content<sup>25</sup> but the nanostructure did not shift from spherical micelles to any other morphology. This fact was confirmed by analytical treatment of images. Figures 3 and 4 show the results of the size distribution and the volume fraction of nanodomains, respectively. Figure 3 shows that the shape of the distributions was modified increasing the size and the number of micelles with the increase of block copolymer content. Similarly, Figure 4 shows the increase in volume fraction of nanodomains with the increasingly addition of block copolymer.

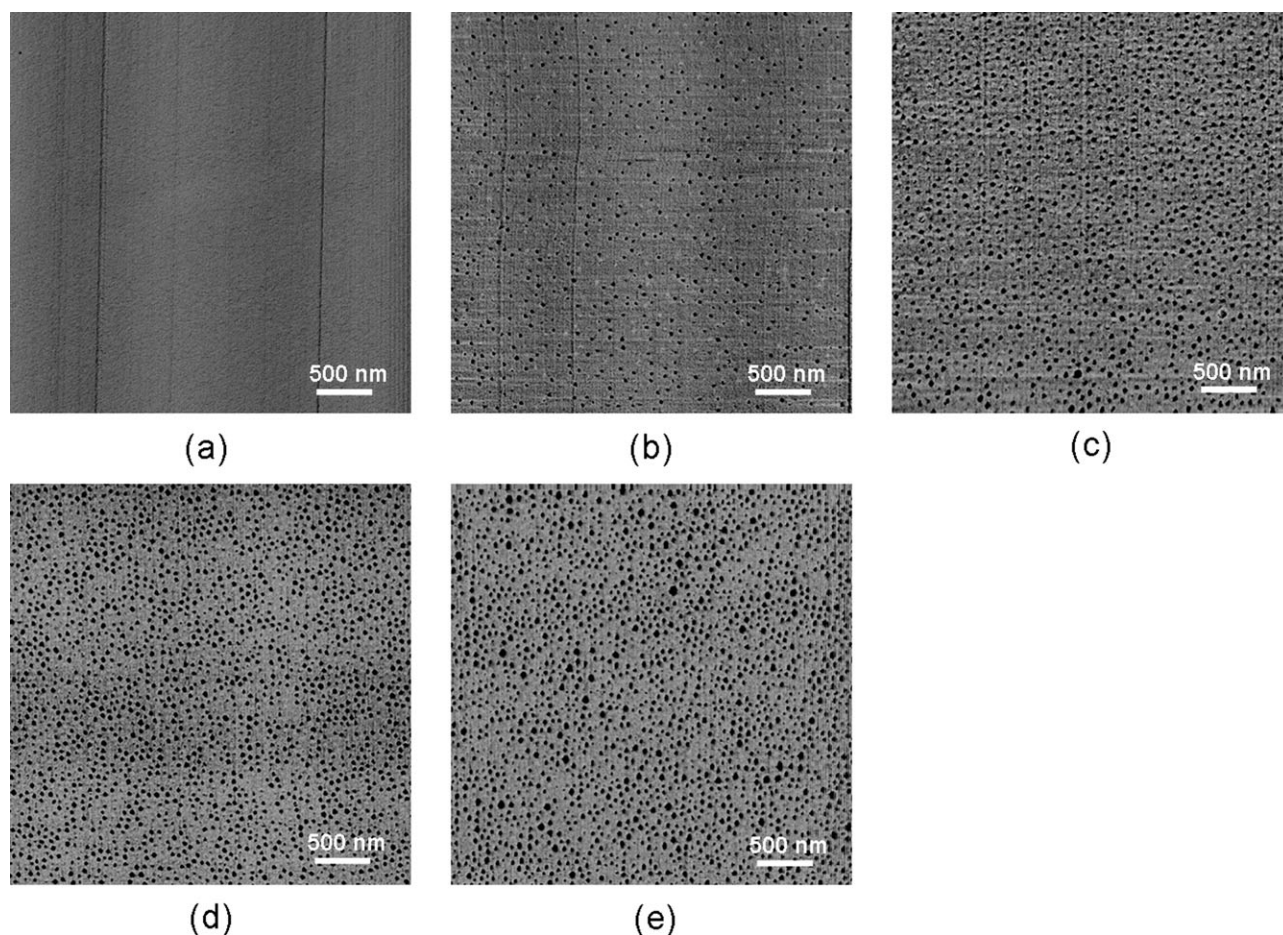


**Figure 2.** TM-AFM phase images ( $3 \times 3 \mu\text{m}^2$ ) of cured DGEBA/MCDEA systems with different PI-*b*-PMMA contents of: (a) 0 wt %, (b) 5 wt %, (c) 10 wt %, (d) 20 wt %, and (e) 30 wt %.

Regarding epoxy/PI-*b*-PMMA/MWCNT composites, the effect of block copolymer on MWCNT dispersion was analyzed, together with their effect on nanostructuring. Figure 5 shows AFM images of epoxy systems modified with different PI-*g*-CNT contents, both with and without PI-*b*-PMMA. When samples without block copolymer were prepared for AFM characterization, huge aggregates were observed with the optical microscope (images not shown here), some of them being larger than  $40 \mu\text{m}$ . As it can be seen from the AFM image in Figure 5(a.I) for the case of the epoxy matrix modified with 0.2 wt % PI-*g*-CNT, just a few CNT were dispersed in the thermoset matrix, the rest remaining as agglomerates.

PI grafting modifies the surface energy of CNT, enhancing wettability and interfacial bonding with nanostructured epoxy matrix. However, from Figure 5 (a.II, b.II), it is clear that, even if the dispersion was better than for pristine CNT, the grafting with PI was not enough to achieve a good dispersion. For each PI-*g*-CNT content, the use of block copolymer could be a good strategy to improve their distribution in the epoxy matrix. It seems that the effect provoked by the adding of block copolymer improved PI-*g*-CNT dispersion in epoxy matrix with respect to nonnanostructured one. In any case, for both systems

with and without block copolymer, a complete dispersion was not achieved, with the presence of agglomerates that increased as the weight fraction of PI-*g*-CNT increased.

Figure 6 shows AFM phase image of epoxy/PI-*g*-CNT with a fixed weight percentage of PI-*b*-PMMA in the resultant composite and the diameter distribution of the spherical micelles. Similar nanostructured morphology to that for the unfilled nanostructured epoxy matrix (Figure 2) was observed, concluding that PI-*g*-CNT did not affect the ability of the block copolymer for nanostructuring in spherical micelle nanodomains. PI-*g*-CNT were randomly oriented along the composite. It is clearly shown that the total number of micelles decreased in both cases with respect to the analogous system modified with 10 wt % of block copolymer without PI-*g*-CNT. PI chains of block copolymer would be located in the vicinity of the CNT, interacting favorably with the polyisoprene grafted to the CNT. Although the blunting of AFM tip due to nanotubes hardness that could lead to a diameter measure error, obtaining lower diameter values than the real micelles diameters, the shape of the diameter distribution showed a decrease in the number of large micelles with respect to the Figure 3(b).

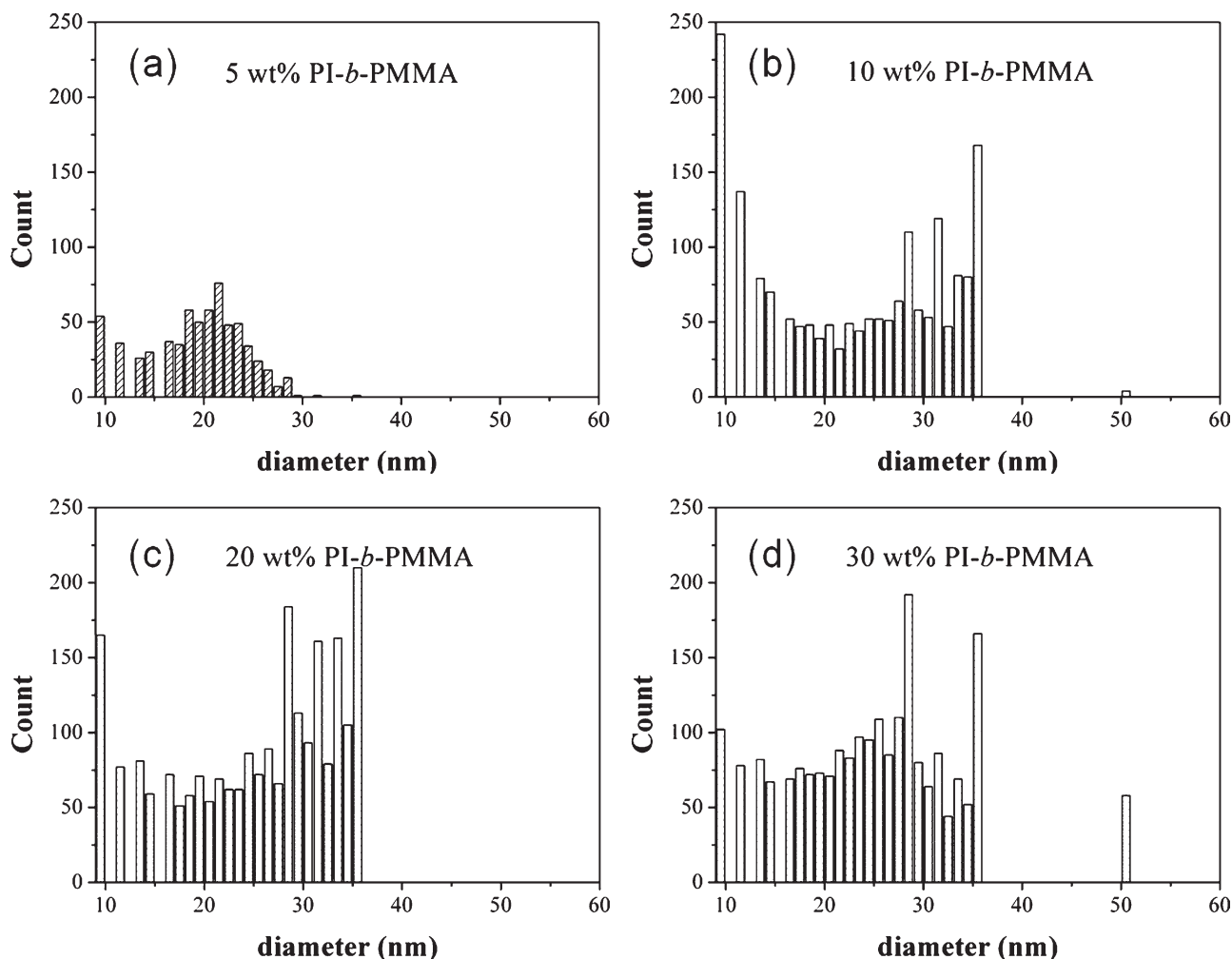


**Figure 3.** Diameter distribution of spherical micelles for nanostructured system modified with block copolymer: (a) 5 wt %; (b) 10 wt %; (c) 20 wt %; and (d) 30 wt %.

### Dynamic Mechanical Properties of Nanocomposites

First, the effect of PI-*b*-PMMA on the glass transition temperature ( $T_g$ ) and storage modulus ( $E'$ ) of epoxy matrix composites was analyzed, as it is shown in Figure 7(a). The  $T_g$  of nanostructured composites decreased with increasing block copolymer content. This phenomenon could be related to the plasticization effect of PMMA chains that were homogeneously dispersed and well interpenetrated into the crosslinked epoxy network.<sup>2,15</sup> On the other hand, storage modulus was shifted toward lower values with block copolymer addition. The reason could be the increment of PI domains in the epoxy network, which are ductile with a  $T_g$  far below room temperature. Thus, PI domains remained as rubbery phase into the final composite.<sup>26,27</sup>

The effect of PI-*g*-CNT on the dynamic mechanical properties of epoxy/PI-*g*-CNT composites without copolymer was also analyzed. Interfacial adhesion and PI-*g*-CNT dispersion in the matrix are two interrelated factors that affect the mechanical properties of nanocomposites. To improve both, the use of grafted-CNT is one of the most useful ways.<sup>16–18</sup> As it is shown in Figure 7(b),  $T_g$  values remained approximately constant at low PI-*g*-CNT contents (<0.5 wt %) for nonnanos-

structured systems. Similar behavior was reported by other authors using different weight percentage of nonfunctionalized MWCNT.<sup>28</sup> However, when PI-*g*-CNT content increased at

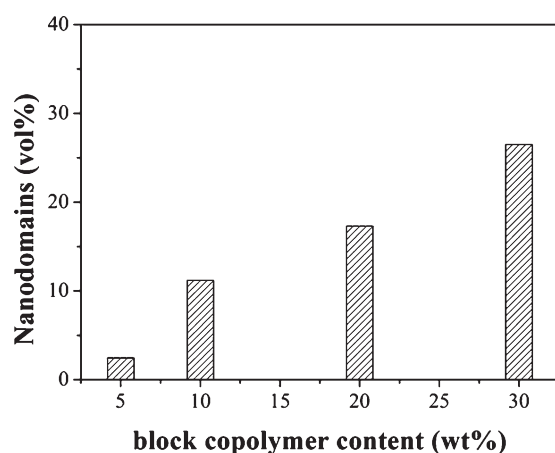


**Figure 4.** Number of micelles per unit area as a function of copolymer content for different diameter ranges: (a) total; (b) small; (c) intermediate; and (d) large.

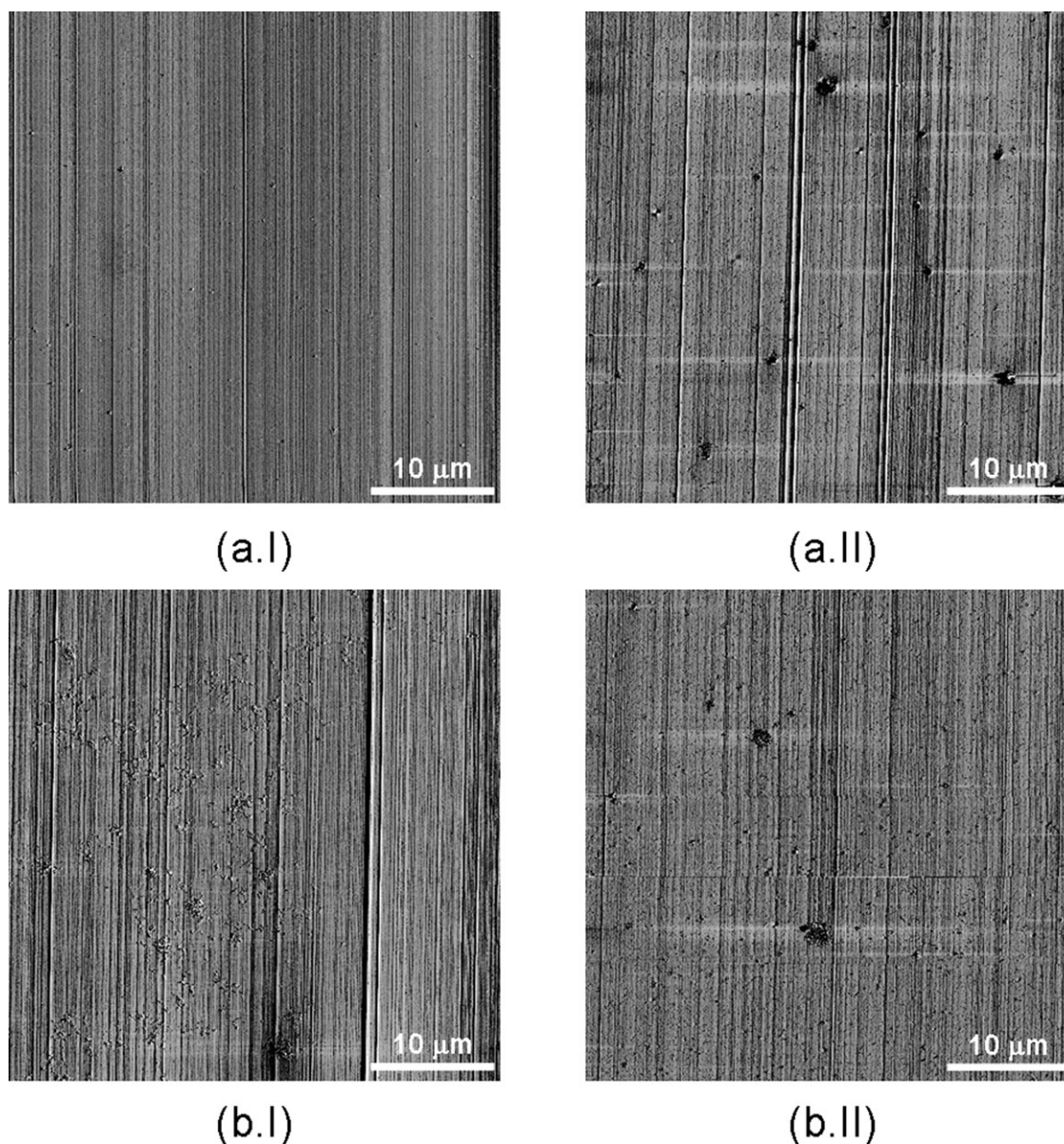


**Figure 5.** TM-AFM phase images ( $40 \times 40 \mu\text{m}$ ) of cured DGEBA/MCDEA systems with different PI-g-CNT contents: (a) 0.2 wt %; (b) 0.5 wt %; (I) without PI-*b*-PMMA, and (II) with 5 wt % PI-*b*-PMMA.

0.5 wt %,  $T_g$  value decreased probably due to the higher amount of PI-g-CNT agglomerates.<sup>28,29</sup> Storage modulus values were higher for the composites containing lower amounts of PI-g-CNT (0.05 and 0.2 wt %) when compared with that of neat epoxy matrix. The increase of the glassy and rubbery modulus with PI-g-CNT content could be due to the stiffness effect around PI-g-CNT.<sup>30</sup>

However, a decrease in the modulus for 0.5 wt % content was observed when compared with those of 0.05 and 0.2 wt % PI-g-CNT, probably related with the presence of a higher amount of agglomerates that reduced the reinforcement effect.<sup>28,29</sup>

To analyze together the effect of both block copolymer and PI-g-CNT on dynamic mechanical behavior, results for epoxy

matrix modified with 5 and 10 wt % PI-*b*-PMMA and several PI-*b*-CNT amounts are shown in Figure 8.

It is interesting to note that for epoxy/PI-*b*-PMMA/PI-g-CNT systems, a better nanoscale dispersion was confirmed by AFM images, even if some agglomerates were still present. This result suggests that the addition of PI-*b*-PMMA lead to a slight increase in storage modulus probably due to the stiffening effect of PI-g-CNT and the lower amount of PI-g-CNT agglomerates,<sup>28,29</sup> even at higher filler weight percentage used (0.5 wt %).

The enhancement of modulus was found to be more significant in the rubbery region probably due to the reduction of mobility of epoxy chains around the PI-g-CNT, which led to increase in thermal stability.<sup>28</sup>

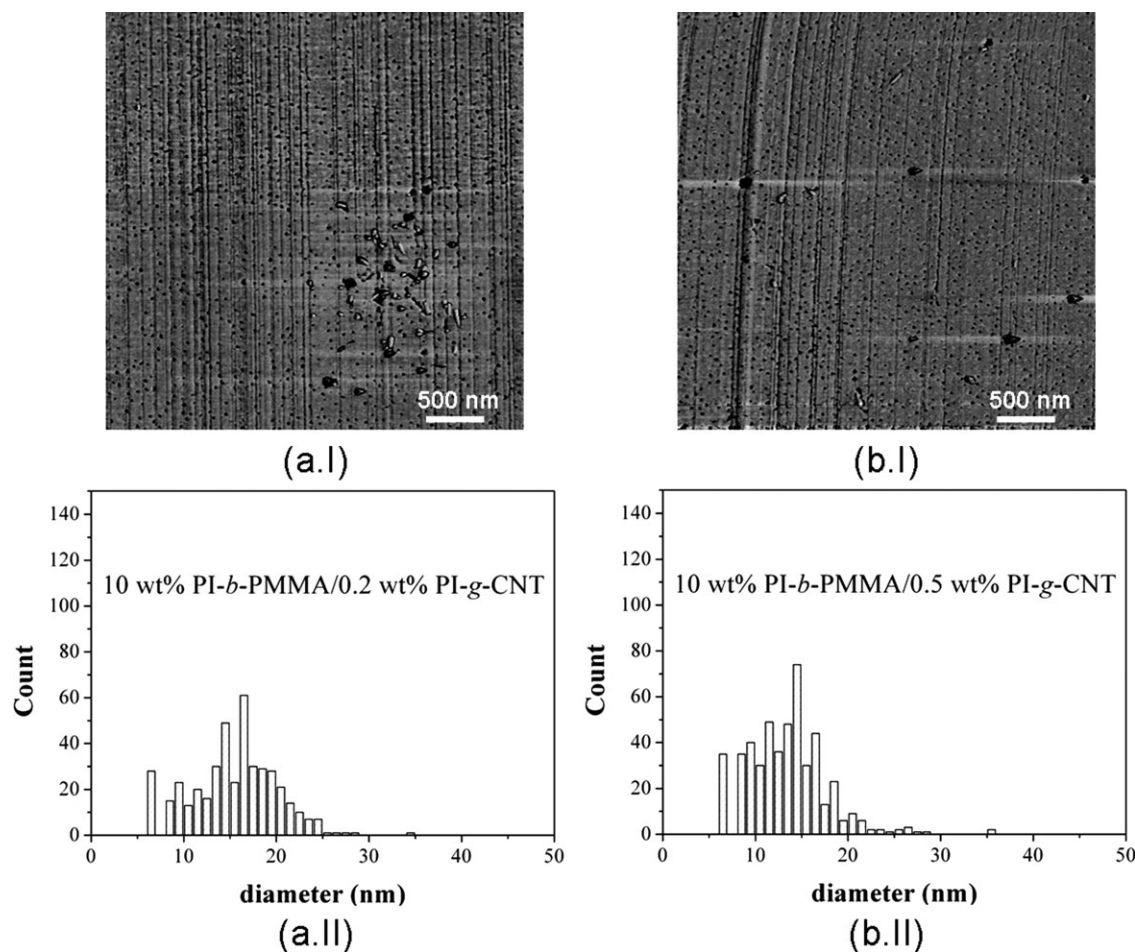


**Figure 6.** TM-AFM phase image ( $3 \times 3 \mu\text{m}^2$ ) and diameter distribution of spherical micelles for nanostructured system with 10 wt % of PI-*b*-PMMA and modified with: (a) 0.2 wt % of PI-*g*-CNT; and (b) 0.5 wt % of PI-*g*-CNT. (I) AFM images; (II) diameter distribution.

Regarding  $T_g$  values, the interactions between better dispersed PI-*g*-CNT and nanostructured epoxy matrix could lead to a slight increase of the  $T_g$  due to the reduction of the molecular mobility of epoxy chains. Other authors found similar behavior for epoxy/CNT composites.<sup>31,32</sup>

### Compression Properties of Nanocomposites

Compressive modulus and yield point were determined by means of compressive-strain test curves at room temperature. Figure 9 shows results obtained for all the systems analyzed. Compressive modulus slightly decreased with PI-*b*-PMMA

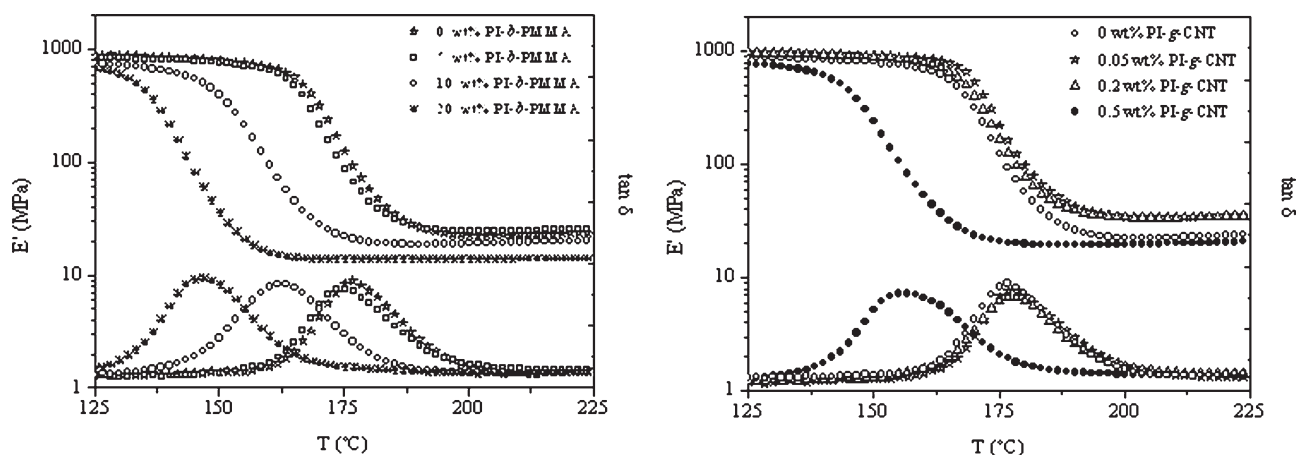


**Figure 7.** Dynamic mechanical curves obtained at 1 Hz for DGEBA/MCDEA systems modified (a) with different PI-*b*-PMMA amounts and (b) with different PI-*g*-CNT amounts.

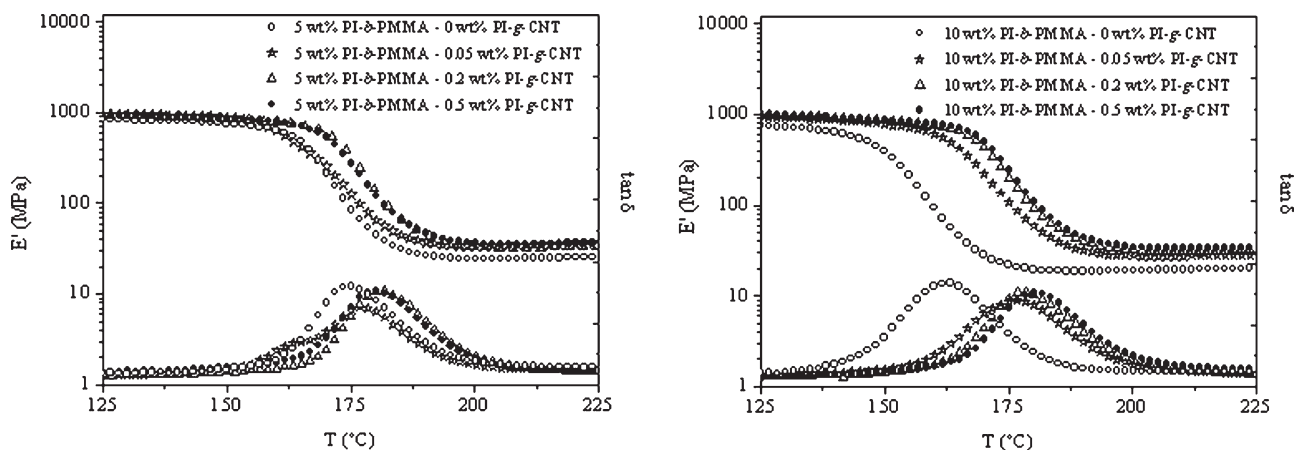


**Figure 8.** Dynamic mechanical curves obtained at 1 Hz for DGEBA/MCDEA systems modified with different PI-g-CNT amounts and: (a) 5 wt % PI-*b*-PMMA; and (b) 10 wt % PI-*b*-PMMA.

content.  $T_g$  of PI domains is below room temperature and as consequence, their stiffness is lower than that of the epoxy network at room temperature.<sup>26,27</sup> For the same copolymer content, the addition PI-g-CNT led to a very slight increase of the modulus within the experimental error and it could be considered that the modulus remained almost constant with PI-g-CNT content. The compressive yield point seemed not to be strongly affected by PI-g-CNT or block copolymer content; this behavior could be due to the strong affinity between grafted PI chains and those of the block copolymer, without necessity of entanglements between them.<sup>7</sup>

## CONCLUSIONS

Nanocomposites based on a epoxy matrix modified with poly(*i*-soprene-*b*-methyl methacrylate) block copolymer and PI-g-CNT were prepared, analyzing obtained morphologies and mechanical properties. The main conclusions that can be extracted from the present work are the following.

Nanostructured epoxy systems were obtained. A micellar morphology was obtained, in which the PI block, immiscible with

the matrix constituted the micelles, whereas the fully miscible PMMA remained in the epoxy phase. The morphologies were not affected by the presence of PI-g-CNT but the number and the size of spherical nanodomains increased with increasing PI-*b*-PMMA content, as was confirmed by analytical treatment of images.

Even if the total dispersion of nanotubes was not obtained and agglomerates were still present in the composites, block copolymer could interact with PI-g-CNT allowing their debundling and consequently improving their dispersion in the host epoxy matrix when compared with those systems without nanostructuring. Consequently, the thermomechanical performance ( $T_g$  or storage modulus values) of the nanocomposites was found to slightly increase by the presence of the dispersed nanofiller when block copolymer was used. For the case of systems without block copolymer,  $T_g$  values remained almost constant and modulus slightly increased for low nanofiller content, whereas for the highest content used both decreased due to the presence of agglomerates. Thus, the nanostructuring of the matrix allowed somehow a better dispersion of nanotubes, with a slight

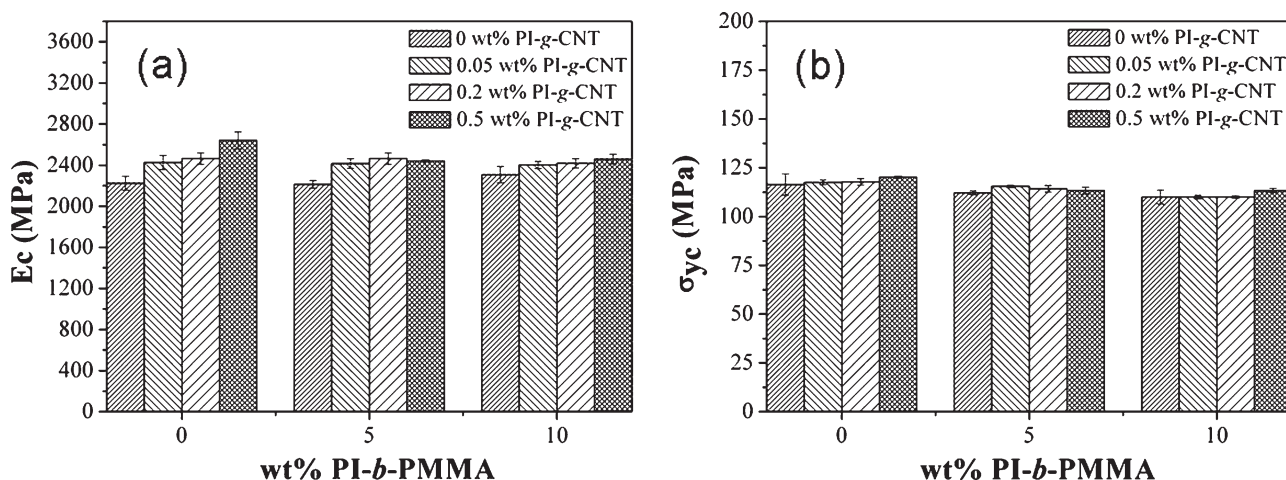


**Figure 9.** Evolution of (a) compressive modulus and (b) compressive yield strength with PI-g-CNT content for DGEBA/MCDEA systems modified with different PI-*b*-PMMA amounts.

increase of  $T_g$  and modulus values, even for the highest content used.

Compressive modulus and strength slightly decreased with the incorporation of PI-*b*-PMMA into neat epoxy matrix. For the same copolymer content, modulus remained almost constant with PI-g-CNT content, with a very slight increase that could be considered within the experimental error. Regarding the compressive yield strength, it appeared almost constant with PI-g-CNT addition for the same amount of block copolymer. This could be attributed to the viscoelastic nature of PI chains grafted on the CNT surface and the affinity between grafted PI chains and those from the block copolymer.

#### ACKNOWLEDGMENT

Authors would like to dedicate this article to the memory of our friend Professor Iñaki Mondragon, who passed away during its preparation. Financial support from the EU (Carbon nanotube confinement strategies to develop novel polymer matrix composites, POCO, FP7-NMP-2007, CP-IP 213939-1), from the Basque Country Government (NanoIker IE11-304, Grupos Consolidados IT-365-07), and from the Ministry of Education and Innovation (MAT 2009-06331) is gratefully acknowledged. Technical and human support provided by SGIker (UPV/EHU, MICINN, GV/EJ, ERDF and ESF) is also acknowledged. Authors would also like to acknowledge A. Avgeropoulos, N. Z. Zafeiropoulos, and D. Katsiannopoulos from the University of Ioannina for the synthesis of PI-*b*-PMMA and PI-g-CNT.

#### REFERENCES

- Mijovic, J.; Shen, M.; Sy, W.; Mondragon, I. *Macromolecules* **2000**, *33*, 5235.
- Ritzenthaler, S.; Court, F.; Girard-Reydet, E.; Leibler, L.; Pascault, J. P. *Macromolecules* **2003**, *36*, 118.
- Larrañaga, M.; Serrano, E.; Martin, M. D.; Tercjak, A.; Kortaberria, G.; de la Caba, K.; Riccardi, C. C.; Mondragon, I. *Polym. Int.* **2007**, *56*, 1392.
- Maiez-Tribut, S.; Pascault, J. F.; Soule, E. R.; Borrajo, J.; Williams, R. J. *Macromolecules* **2007**, *40*, 1268.
- Fan, W.; Zheng, S. *Polymer* **2008**, *49*, 3157.
- Loos, M. R.; Yang, J.; Feke, D. L.; Manas-Zloczower, I. *Comp. Sci. Tech.* **2012**, *72*, 482.
- Albuerne, J.; Boschetti-de-Fierro, A.; Abetz, C.; Fierro, D.; Abetz, V. *Adv. Eng. Mater.* **2011**, *13*, 803.
- Bockstaller, M. R.; Mickiewicz, R. A.; Thomas, E. L. *Adv. Mater.* **2005**, *17*, 1331.
- Peponi, L.; Valentini, L.; Torre, L.; Mondragon, I.; Kenny, J. M. *Carbon* **2009**, *47*, 2474.
- Lo, C. -T.; Lee, B.; Pol, V. G.; Dietz Rago, N. L.; Seifert, S.; Winans, R. E.; Thiyagarajan, P. *Macromolecules* **2007**, *40*, 8302.
- Park, I.; Lee, W.; Kim, J.; Park, M.; Lee, H. *Sensors Actuat. B-Chem.* **2007**, *126*, 301.
- Schillén, K.; Yekta, A.; Ni, S.; Farinha, J. P. S.; Winnik, M. A. *J. Phys. Chem. B* **1999**, *103*, 9090.
- Werkhoven, T. M.; Mulder, F. M.; Zune, C.; Jérôme, R.; de Groot, H. J. M. *Macromol. Chem. Phys.* **2003**, *204*, 46.
- Heurtefeu, B.; Oriou, J.; Ibarboure, E.; Cloutet, E.; Cramail, H. *New J. Chem.* **2011**, *35*, 2322.
- Ritzenthaler, S.; Girard-Reydet, E.; Pascault, J. P. *Polymer* **2000**, *41*, 6375.
- Rebizant, V.; Venet, A. -S.; Tournilhac, F.; Girard-Reydet, E.; Navarro, C.; Pascault, J. P.; Leibler, L. *Macromolecules* **2004**, *37*, 8017.
- Wu, J.; Thio, Y. S.; Bates, F. S. *J. Polym. Sci. Part B: Polym. Phys.* **2005**, *43*, 1950.
- Hydro, R. M.; Pearson, R. A. *J. Polym. Sci. Part B: Polym. Phys.* **2007**, *45*, 1470.
- Bashar, M.; Sundararaj, U.; Mertiny, P. *Express Polym. Lett.* **2011**, *5*, 882.
- Coleman, J. M.; Khan, U.; Gunko, Y. K. *Adv. Mater.* **2006**, *18*, 689.
- Hwang, G. L.; Shieh, Y. -T.; Hwang, K. C. *Adv. Funct. Mater.* **2004**, *14*, 487.
- Nayak, R. R.; Lee, K. Y.; Shanmugaraj, A. M.; Ryu, S. H. *Eur. Polym. J.* **2007**, *43*, 4916.
- Fragneaud, B.; Masenelli-Varlot, K.; Gonzalez-Montiel, A.; Terrones, M.; Cavallé, J. Y. *Compos. Sci. Technol.* **2008**, *68*, 3265.
- Litina, K.; Miriouni, A.; Gournis, D.; Karakassides, M.; Georgiou, N.; Klontzas, E.; Ntoukas, E.; Avgeropoulos, A. *Eur. Polym. J.* **2006**, *42*, 2098.
- Ramos, J. A.; Espósito, L. H.; Fernández, R.; Zalakain, I.; Goyanes, S.; Avgeropoulos, A.; Zafeiropoulos, N. E.; Kortaberria, G.; Mondragon, I. *Macromolecules* **2012**, *45*, 1483.
- Tonpheng, B.; Yu, J.; Andersson, B. M.; Andersson, O. *Macromolecules* **2010**, *43*, 7680.
- Lopes, S. I. C.; Gonçualves da Silva, A. M. P. S.; Brogueira, P.; Picüarra, S.; Martinho, J. M. G. *Langmuir* **2007**, *23*, 9310.
- Gojny, F. H.; Schulte, K. *Compos. Sci. Technol.* **2004**, *64*, 2303.
- Ma, P. C.; Mo, S. Y.; Tang, B. Z.; Kim, J. K. *Carbon* **2010**, *48*, 1824.
- Prolongo, S. G.; Campo, M.; Gude, M. R.; Chaos-Morán, R.; Ureña, A. *Compos. Sci. Technol.* **2009**, *69*, 349.
- Teng, C. -C.; Ma, C. -C. M.; Yang, S. -Y.; Chiou, K. -C.; Lee, T. -M.; Chiang, C. -L. *J. Appl. Polym. Sci.* **2012**, *123*, 888.
- Cho, J.; Daniel, I. M.; Dikin, D. A. *Compos. Part A: Appl. Sci.* **2008**, *39*, 1844.